CRYSTAL GROWTH & DESIGN

Communication

pubs.acs.org/crystal

Crystal Growth of the Perovskite Semiconductor $CsPbBr_3$: A New Material for High-Energy Radiation Detection

Constantinos C. Stoumpos,[†] Christos D. Malliakas,[†] John A. Peters,[§] Zhifu Liu,[§] Maria Sebastian,[§] Jino Im,[⊥] Thomas C. Chasapis,[‡] Arief C. Wibowo,[†] Duck Young Chung,[†] Arthur J. Freeman,[⊥] Bruce W. Wessels,[§] and Mercouri G. Kanatzidis*[,†,‡]

[†]Materials Science Division, Argonne National Laboratory, Argonne, Illinois 60439, United States

[‡]Department of Chemistry, [§]Department of Materials Science and Engineering, and [⊥]Department of Physics and Astronomy, Northwestern University, Evanston, Illinois 60208, United States

Supporting Information

ABSTRACT: The synthesis, crystal growth, and structural and optoelectronic characterization has been carried out for the perovskite compound $CsPbBr_3$. This compound is a direct band gap semiconductor which meets most of the requirements for successful detection of X- and γ-ray radiation, such as high attenuation, high resistivity, and significant photoconductivity response, with detector resolution comparable to that of commercial, state-of-the-art materials. A structural phase transition which occurs during crystal growth at higher temperature does not seem to affect its crystal quality. Its $\mu\tau$ product for both hole and electron carriers is approximately equal. The $\mu\tau$ product for electrons is comparable to cadmium zinc telluride (CZT) and that for holes is 10 times higher than CZT.

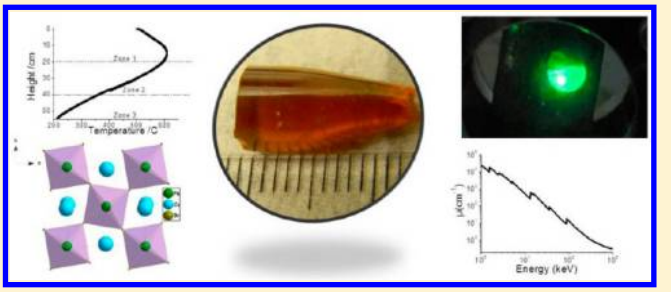

X- and γ-ray detectors operating at room temperature constitute an important aspect of the current technological era, since the need for radiation detection is becoming increasingly important not only for scientific purposes but also for applications related to the welfare of modern society, such as nuclear medicine imaging, environmental radioactivity monitoring, and spacecraft and national security equipment to name a few.[1] Semiconductors are materials of great interest for the manufacture of X- and γ-ray radiation detectors because they promise high spectral resolution and high sensitivity. Such materials have intrinsically large energy gap (E_g), in the range of 1.6−3.0 eV, which reduces the spectral noise arising from thermally activated carrier "hopping" (dark current). Additional major material requirements are high resistivity, of the order of GΩ cm or higher, and a high attenuation coefficient, which is achieved in compounds containing high atomic number elements. Generally, it is a challenge to identify such materials because most heavy metal semiconducting compounds tend to possess narrow energy gaps. The leading detector material is the $Cd_{0.9}Zn_{0.1}Te$ (CZT) composition of the $Cd_{1-x}Zn_xTe$ solid solution, which has an E_g of 1.65 eV, a high density, and a high resistivity. These properties are expressed by the so-called figure of merit of detector materials, namely the mobility lifetime product ($\mu\tau$), as obtained from photoconductivity measurements. Typical $\mu\tau$ values for CZT are close to 1×10^{-3} cm^2/V, although values as high as 10^{-2} cm^2/V have been reported.[1b,c,2] Another promising set of compounds for detector applications, currently under development, is the binary compound TlBr and the related $TlBr_{1-x}I_x$ solid solution which display some advantages over CZT, such as higher density and simpler crystal growth conditions.[3] Optimized $\mu\tau$ values for TlBr together with CZT lie in the 10^{-3} cm^2/V region, which is the benchmark for radiation detection. However, crystal growth of CZT has been known to be problematic due to its solid solution nature, which generates inhomogeneity in composition, as well as the formation of Te precipitates during crystal growth.[2c] TlBr is very soft and tends to suffer from polarization effects.[4]

Following our ongoing interest in discovering alternative compounds suitable for high energy radiation detection,[5] we turned our attention to heavy metal semiconductors which favor a wide band gap, such as chalcogenides,[5a,c−e] chalcohalides,[5b,6] and halides. In general, binary halide compounds despite their promising optoelectronic properties have not yet succeeded as detector materials due to their poor mechanical properties and low $\mu\tau$. Layered compounds such as PbI_2[7] and BiI_3[8] readily deform on application of pressure due to the van der Waals gap between the layers, generating defects and dislocations which negatively impact the detector performance. Another promising compound, HgI_2, suffers from a structural phase transition at relatively low temperatures and precludes the growth of large single crystals.[9] Here, we report on $CsPbBr_3$, a compound with better mechanical stability and

Received: April 27, 2013
Revised: May 29, 2013
Published: June 3, 2013

favorable optoelectronic properties. This compound crystallizes in the three-dimensional (3D) perovskite structural type, thus lacking van der Waals gaps. Additionally, the linear attenuation coefficient, calculated using the XCOM application by NIST,[10] is comparable to CZT throughout the high-energy radiation spectrum (Figure 1).

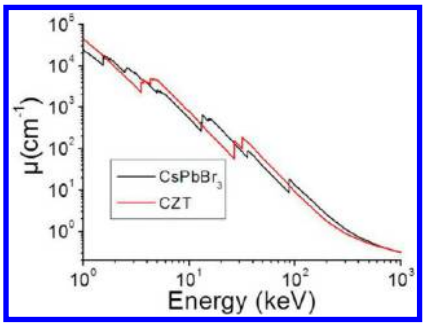

Figure 1. Calculated attenuation coefficients for CZT and $CsPbBr_3$ in the 1−1000 keV energy range.

The properties of $CsPbBr_3$ have been studied more than 50 years ago,[11] but this material has not been examined as a possible X-ray and γ-ray detector. Nevertheless, it has subsequently attracted much interest because of its unusual structural,[12] optical,[13] electronic,[14] and charge transport[15] properties. The present work is focused on synthesis and crystal growth of $CsPbBr_3$ and characterization of its fundamental photoconductivity properties in order to evaluate the eligibility of the compound as a detector. Here, we demonstrate X-ray photoresponse observed from a Ag radiation source.

$CsPbBr_3$ crystallizes in the orthorhombic (*Pnma*) space group, adopting a distorted perovskite structure, as determined by the single-crystal diffraction at room temperature,[16] where the $\{PbBr_6\}^{4-}$ octahedra are tilted with respect to the orthogonal geometry of the ideal perovskite structure (Figure 2a). The distortion occurs through two successive phase transitions at 88 and 130 °C, transforming the crystal structure to tetragonal (*P*4/*mbm*) and cubic (*Pm*-3*m*), respectively. An immediate effect of the structural transition is the formation of pseudomerohedral twin domains, which is detected by single-crystal structural refinement[17] and typically occurs along the [010] crystallographic direction. Twinning is also supported by spectroscopic measurements where the phonon absorption corresponding to the Pb−Br vibrations displays a broad distribution (Figure S1 of the Supporting Information). The phase transitions were studied using temperature-dependent high-resolution X-ray powder diffraction, where the changes in the crystal symmetry were structurally refined (Figure 2b).[18] The thermal expansion and the branching of the lattice parameters were thus determined. The volumetric expansion increases linearly with temperature, unaffected by the phase transitions, producing a value of 1.2×10^{-4} K^{-1} for the thermal expansion coefficient (Figure 2c). On the other hand, the individual lattice parameters show a nonlinear expansion (Figure 2d), in excellent agreement with previously reported results.[12d] In order to better represent the changes in the unit cell along the crystallographic *c* axis, the space group was transformed to *Pbnm* from *Pnma* by simple rearrangement of the crystallographic axes.

$CsPbBr_3$ is readily prepared by reacting equimolar amounts of CsBr and $PbBr_2$ in a sealed fused silica ampule at 600 °C or by mixing equimolar solutions of $PbBr_2$ and CsBr in concentrated aqueous hydrobromic acid [48% HBr(aq)],

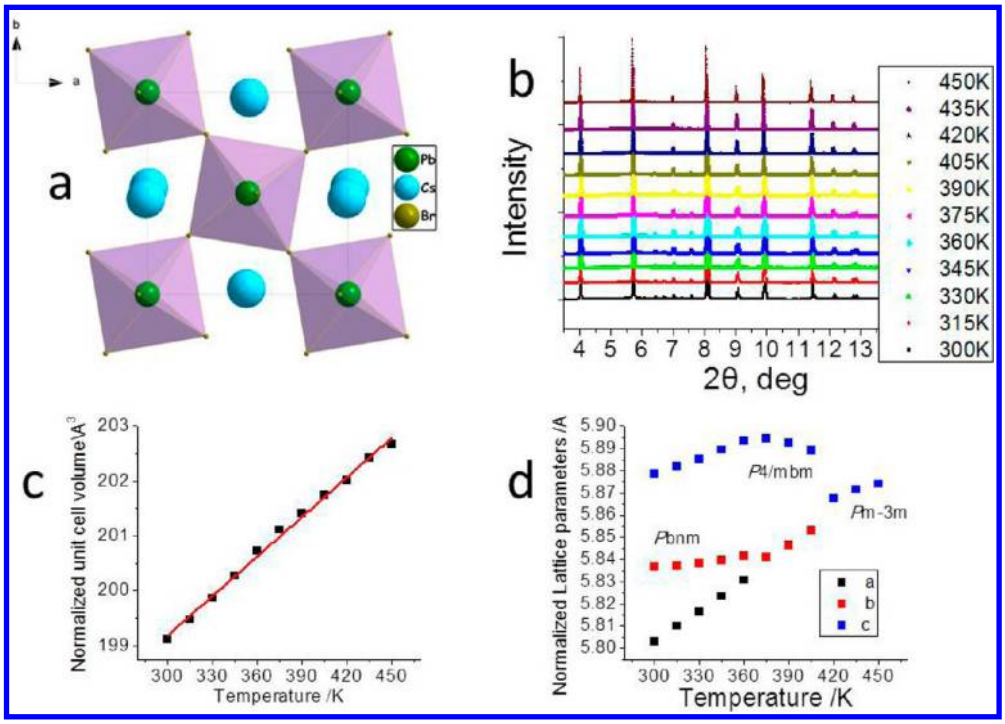

Figure 2. (a) Crystal structure of $CsPbBr_3$ in the *Pbnm* space group modification. (b) Temperature-dependence powder diffraction study of $CsPbBr_3$ using a synchrotron radiation of λ = 0.41361 Å. (c) Volumetric expansion of $CsPbBr_3$ as a function of temperature. (d) Branching of the lattice parameters for $CsPbBr_3$ as a function of temperature.

dx.doi.org/10.1021/cg400645t | *Cryst. Growth Des.* 2013, 13, 2722−2727

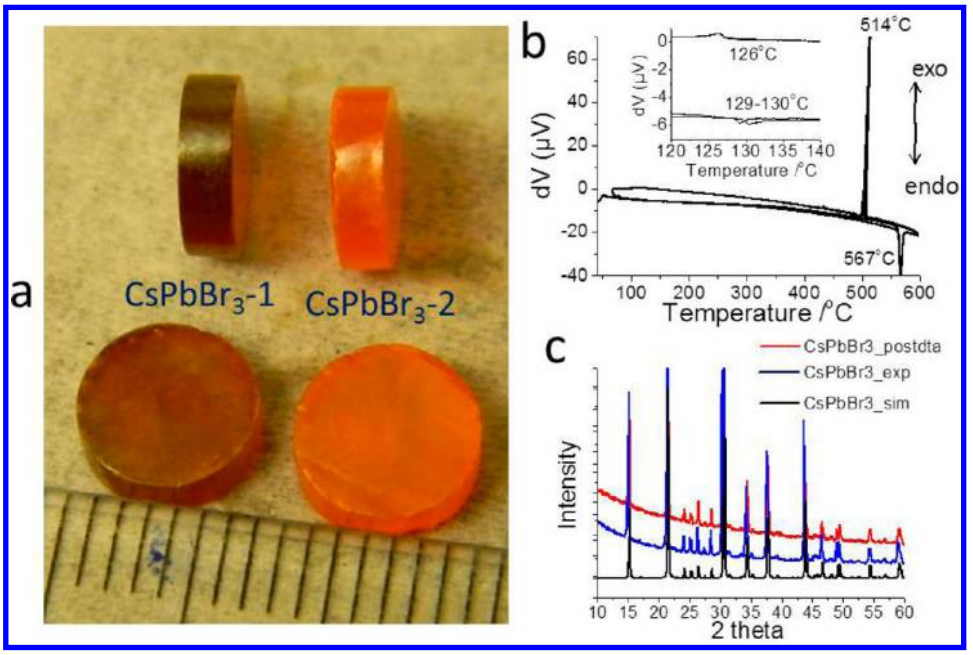

Figure 3. (a) Photograph of the single-crystal specimens $CsPbBr_3$-1 and $CsPbBr_3$-2. (b) DTA plot of $CsPbBr_3$ showing the crystallization/melting. Inset: magnification of the 120−140 K region of the DTA graph showing the thermal response of the cubic-to-tetragonal phase transition and (c) the recorded powder patterns before and after the thermal treatment, showing identical diffraction.

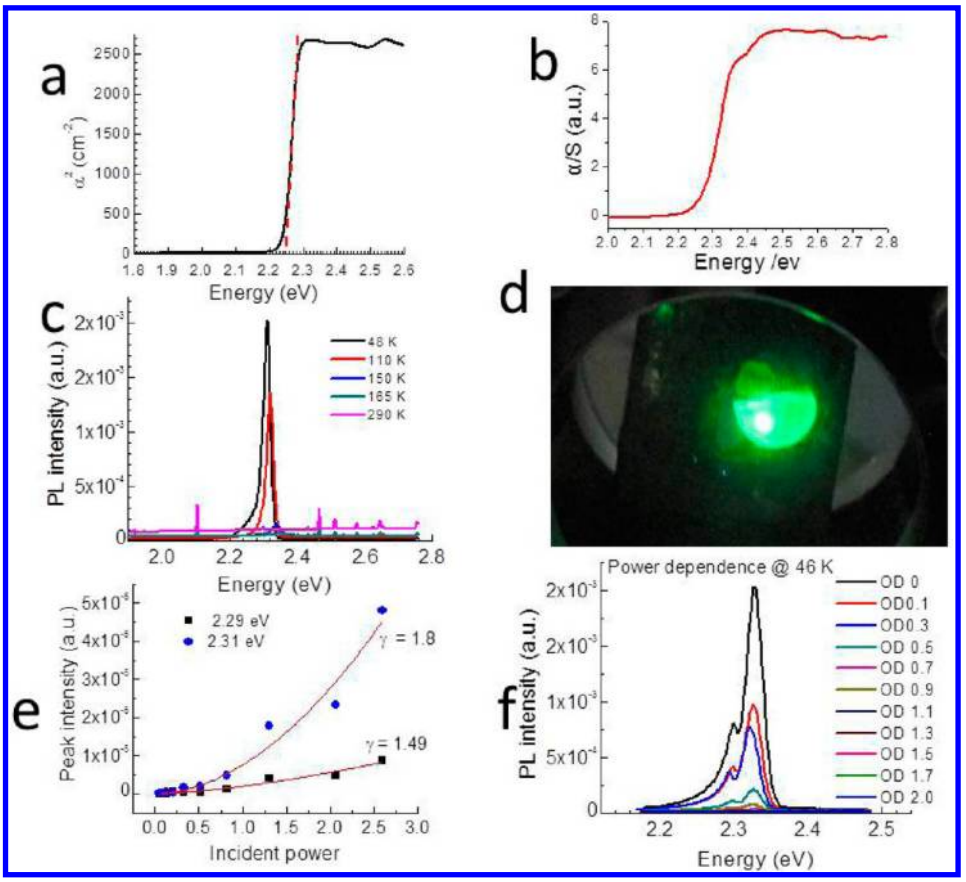

Figure 4. (a) Single-crystal transmission spectrum of $CsPbBr_3$. (b) Diffuse reflectance spectrum of a polycrystalline sample of $CsPbBr_3$. (c) PL emission spectrum of a single crystal of $CsPbBr_3$ as a function of temperature. (d) A photograph of the strong PL emission of a $CsPbBr_3$ specimen at 46 K. The PL-emission intensity dependence on the excitation beam intensity plotted vs (e) incident power and (f) energy, respectively, at 46 K for the same specimen of $CsPbBr_3$ shown in (d).

respectively. Crystal growth of a 7 mm diameter crystal ingot was achieved by the vertical Bridgman method using a three-zone furnace, for a translation speed of 10.0 mm/h for a set temperature profile (Figure S2 of the Supporting Information).

dx.doi.org/10.1021/cg400645t | Cryst. Growth Des. 2013, 13, 2722−2727

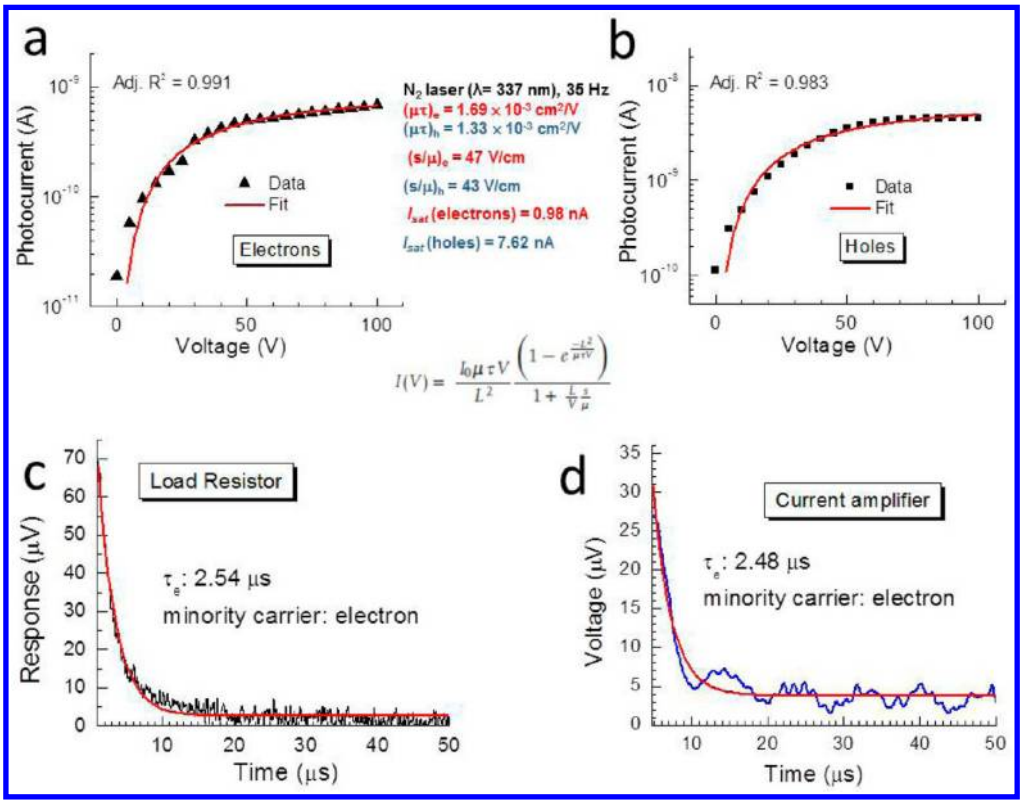

Figure 5. Photoconductivity data from samples of $CsPbBr_3$ ($\rho \approx 1.42$ GΩ cm) for (a) electrons and (b) holes. The fitting of the data is based on the Many equation. (c, d) Electron lifetime measured for $CsPbBr_3$-1, using a load resistor and a current amplifier setup.

A typical charge of 6 g $CsPbBr_3$ was loaded in a 9 mm o.d. fused silica ampule and sealed under a 10^{-4} mbar pressure. The compound melts at ~567 °C and crystallizes at ~514 °C, as determined by differential thermal analysis (DTA) experiments. The compound melts congruently as confirmed by X-ray diffraction and DTA results (Figure 3, panels b and c). Of the two-phase transitions, only the one at 130 °C is resolved, which suggests that the tetragonal-to-cubic phase transition is a first order, whereas the orthorhombic-to-tetragonal one is a second order. The transition is reversible and as shown below it appears to have no impact on crystal quality or any of its properties.

Two individually grown crystal batches were investigated where $CsPbBr_3$ was prepared using commercially available 5N grade $PbBr_2$ ($CsPbBr_3$-1) and freshly precipitated and dried $PbBr_2$ ($CsPbBr_3$-2) (obtained from mixing aqueous solutions of $Pb(NO_3)_2$ and KBr in a stoichiometric ratio). CsBr was of 5 N purity in both cases. Specimens for characterization were prepared by cutting the grown crystals obtained by the procedure above and polished and etched in concentrated HBr. Resistivity measurements were initially used to evaluate the quality/purity of the crystals. The measurements were conducted in a guarded setup which minimized leakage current by application of voltage (up to 300 V) on the parallel faces of the coins using a spring-loaded sample holder. The sample $CsPbBr_3$-1 displayed a resistivity of ~1 GΩ cm, which is close to that of its previously reported value, whereas $CsPbBr_3$-2 displayed a much larger resistivity of 343 GΩ cm. Photographs and the I–V plots of the processed specimens are shown in Figure 3a and Figure S3 of the Supporting Information, respectively.

Optical absorption and emission properties for $CsPbBr_3$ were studied as a part of our assessment as a detector material. Absorption spectra recorded in an etched and polished single-crystal specimen in transmission mode (Figure 4a) and in a powdered polycrystalline sample of $CsPbBr_3$ in diffuse reflectance mode (Figure 4b) show similar behavior, suggesting that the compound is a direct band gap semiconductor with E_g = 2.25 eV at room temperature. Band structure calculations for the orthorhombic, ambient temperature phase (Figure S4 of the Supporting Information), as well as previously reported calculations for the cubic, high-temperature phase confirm the direct nature of the band gap.[14a,19] The effective mass, m_e,of the carriers was calculated to be $0.23m_e$ for both holes and electrons at room temperature (orthorhombic phase). A detailed analysis of the theoretical calculation will be reported elsewhere. The extra feature of the diffuse reflectance spectrum is associated with strongly bound excitons present in the material. This becomes evident upon collection of the emission spectra (cw He–Cd laser, 325 nm) of $CsPbBr_3$, where a green photoluminescence (PL) emission results from two different wavelengths. At 46 K, two emission peaks are observed at 2.29 and 2.31 eV, respectively. The PL dependence, measured as a function of temperature, shows a dramatic increase in PL intensity starting with a weak signal at room temperature to a very bright one at 46 K (Figure 4, panels c and d). The origin of the PL emission was tracked down by means of power dependence measurements by varying the optical density (transmittance) of the excitation beam at 46 K, where the highest PL intensity is observed (Figure 4, panels e and f). Analysis of the PL peak intensity (I) versus incident beam intensity (F) displays a power law dependence ($I \alpha F^{\gamma}$) for both the 2.29 and the 2.31 eV peaks. The value of the exponential

dx.doi.org/10.1021/cg400645t | Cryst. Growth Des. 2013, 13, 2722–2727

coefficient γ lies between $1 < \gamma < 2$, which is indicative of PL-emission through strongly bound excitons.[20]

Photoconductivity measurements on $CsPbBr_3$ (specimen $CsPbBr_3$-1) suggest it to be a highly photoresponsive material, as expressed by the $\mu\tau$ product, extracted using the Many equation.[21] The estimated $\mu\tau$ product is 1.7×10^{-3} cm^2/V and 1.3×10^{-3} cm^2/V for electrons and holes, respectively (Figure 5, panels a and b). These are remarkably high $\mu\tau$ values and are consistent with the theoretical calculations which predict small and equal effective mass for both charge carriers, implying high mobilities in this material. These values are comparable to those of the commercially available CZT [in this case, electrons have a high $(\mu\tau)_e$, while holes have a significantly lower $(\mu\tau)_h$] or the emerging binary compound TlBr, and thus $CsPbBr_3$ may be a promising candidate for γ-ray detection. Moreover, the fact that both electrons and holes have $\mu\tau$ products of the same order of magnitude renders their incorporation into devices much more feasible since no special engineering methodologies are required for patching mismatches between holes and carriers.[22] The origin of such high $\mu\tau$ products of $CsPbBr_3$ was sought by measuring the relaxation time of the minority carriers, which in this case are the electrons. A very high relaxation time is observed, of the order of a few microseconds. The measurement was carried out consistently using two independent experimental setups producing almost identical values of ~2.5 μs (Figure 5, panels c and d). This number also implies that the mobility of electrons in $CsPbBr_3$ is about 1000 $cm^2/(V\ s)$, which is comparable to that of Si.[23] Both μ_e and τ_e values are very much comparable with those from the recent measurements on CZT, using the transient pulse technique.[24]

On the basis of the photoconductivity results, we performed a direct evaluation of the material as a detector. For this purpose, an unfiltered Ag radiation source (λ = 0.5742 Å, 21.59 keV) was employed. The power settings used were 40 kV/18 mA (0.72 kW). The measurement was carried out by employing a positive bias of 450 V and exposing the sample (specimen $CsPbBr_3$-2, 2.1 mm thick 7 mm diameter) in the beam path for 15 min. A sample of commercial CZT ($5 \times 5 \times 5$ mm^3 cube) was exposed to the beam under the same bias for 5 min. Preliminary results indicate that $CsPbBr_3$ has a significant X-ray response, displaying a signal resolution equivalent to that of CZT, being able to resolve the K_α and K_β peaks. The sensitivity of the response corresponds to approximately 1% of the commercial CZT detector (Figure S5 of the Supporting Information).

In conclusion, we propose $CsPbBr_3$ as a promising candidate material for X- and γ-ray radiation detection. This compound is a direct band gap semiconductor which meets most of the requirements for successful detection, such as high attenuation, high resistivity, and significant photoconductivity response, with resolution comparable to that of commercial, state-of-the-art materials. A structural phase transition, which occurs during crystal growth, does not seem to affect its crystal quality. Its $\mu\tau$ product, a property that facilitates charge collection, is approximately equal for both hole and electron carriers, which could make it easy to fabricate a practical room temperature detector.

■ ASSOCIATED CONTENT

Supporting Information

Synthesis, crystal growth, and processing of $CsPbBr_3$, photoluminescence and photoconductivity measurements, charge transport and detector properties; IR and Raman spectra (Figure S1), furnace temperature profile (Figure S2), I–V characteristic plots (Figure S3), band structure calculations (Figure S4) and the X-ray spectrum of $CsPbBr_3$ (vs CZT) (Figure S5). A cif file of the orthorhombic structure is included. This material is available free of charge via the Internet at http://pubs.acs.org.

■ AUTHOR INFORMATION

Corresponding Author

*E-mail: m-kanatzidis@northwestern.edu. Tel: 847-467-1541. Fax: 847-491-5937.

Notes

The authors declare no competing financial interest.

■ ACKNOWLEDGMENTS

This work is supported by the office of Nonproliferation and Verification Research and Development under the National Nuclear Security Administration of the U.S. Department of Energy under Contract DE-AC02-06CH11357. Use of the Advanced Photon Source at Argonne National Laboratory was supported by the U.S. Department of Energy, Office of Science, Office of Basic Energy Sciences. J.A.P, Z.L., A.J.F., and B.W.W acknowledge support from DTRA under Grant HDTRA1-09-1-0044.

■ REFERENCES

(1) (a) Ramsey, B. D. *Nuclear Science Symposium Conference Record*, 2001 IEEE Nuclear Science Symposium, San Diego, CA, Nov 4–10, 2001; IEEE: New Brunswick, NJ, Vol. *4*, p 2377. (b) Camarda, G. S.; Bolotnikov, A. E.; Cui, Y.; Hossain, A.; Kohman, K. T.; James, R. B. In *Systems, Applications and Technology Conference LISAT2007*, The 3rd Annual Conference on Long Island Systems, Applications and Technology, Farmingdale, NY, May 4, 2007; IEEE: New Brunswick, NJ, p 1. (c) Del Sordo, S.; Abbene, L.; Caroli, E.; Mancini, A. M.; Zappettini, A.; Ubertini, P. *IEEE Sens. J.* **2009**, *9*, 3491. (d) Rahman, R.; Plater, A. J.; Nolan, P. J.; Appleby, P. G. *Radiat. Prot. Dosim.* **2013**, *154*, 477–482.

(2) (a) Chu, M.; Terterian, S.; Ting, D.; James, R. B.; Szawlowski, M.; Visser, G. J. 2003, 237; (b) Amman, M.; Lee, J. S.; Luke, P. N.; Chen, H.; Awadalla, S. A.; Redden, R.; Bindley, G. *IEEE Trans. Nucl. Sci.* **2009**, *56*, 795. (c) Bolotnikov, A. E.; Babalola, S.; Camarda, G. S.; Cui, Y.; Egarievwe, S. U.; Hossain, A.; Yang, G.; James, R. B. In *34th Annual GOMACTech Conference*, Brookhaven National Laboratory, Upton, NY, Mar 16–19, 2009; NTIS: Springfield, VA, 2009; OSTI ID: 950455. (d) Bolotnikov, A. E.; Camarda, G. S.; Cui, Y.; Hossain, A.; Yang, G.; Yao, H. W.; James, R. B. *IEEE Trans. Nucl. Sci.* **2009**, *56*, 791. (e) Washington, A. L.; Teague, L. C.; Duff, M. C.; Burger, A.; Groza, M.; Buliga, V. *J. Appl. Phys.* **2012**, *111*, 113715.

(3) (a) Kim, H.; Churilov, A.; Ciampi, G.; Cirignano, L.; Higgins, W.; Kim, S.; O'Dougherty, P.; Olschner, F.; Shah, K. *Nucl. Instrum. Methods Phys. Res., Sect. A* **2011**, *629*, 192. (b) Bishop, S. R.; Tuller, H. L.; Ciampi, G.; Higgins, W.; Engel, J.; Churilov, A.; Shah, K. S. *Phys. Chem. Chem. Phys.* **2012**, *14*, 10160. (c) Hadong, K.; Kargar, A.; Cirignano, L.; Churilov, A.; Ciampi, G.; Higgins, W.; Olschner, F.; Kanai, S. *IEEE Trans. Nucl. Sci.* **2012**, *59*, 243. (d) Hitomi, K.; Tada, T.; Onodera, T.; Kim, S.; Xu, Y.; Shoji, T.; Ishii, K. *IEEE Trans. Nucl. Sci.* **2012**, 1. (e) Nakhostin, M.; Hitomi, K. *Nucl. Instrum. Methods Phys. Res., Sect. A* **2012**, *675*, 47.

(4) Donmez, B.; Thrall, C. L.; Zhong, H.; Cirignano, L. J.; Hadong, K.; Shah, K. S. In *Nuclear Science Symposium Conference Record*, 2010 IEEE Nuclear Science Symposium, Knoxville, TN, Oct 30–Nov 6, 2010, IEEE: New Brunswick, NJ, p 3773.

(5) (a) Androulakis, J.; Peter, S. C.; Li, H.; Malliakas, C. D.; Peters, J. A.; Liu, Z.; Wessels, B. W.; Song, J.-H.; Jin, H.; Freeman, A. J.; Kanatzidis, M. G. *Adv. Mater.* **2011**, *23*, 4163. (b) Johnsen, S.; Liu, Z.; Peters, J. A.; Song, J.-H.; Nguyen, S.; Malliakas, C. D.; Jin, H.;

Freeman, A. J.; Wessels, B. W.; Kanatzidis, M. G. *J. Am. Chem. Soc.* **2011**, *133*, 10030. (c) Johnsen, S.; Liu, Z.; Peters, J. A.; Song, J.-H.; Peter, S. C.; Malliakas, C. D.; Cho, N. K.; Jin, H.; Freeman, A. J.; Wessels, B. W.; Kanatzidis, M. G. *Chem. Mater.* **2011**, *23*, 3120. (d) Li, H.; Peters, J. A.; Liu, Z.; Sebastian, M.; Malliakas, C. D.; Androulakis, J.; Zhao, L.; Chung, I.; Nguyen, S. L.; Johnsen, S.; Wessels, B. W.; Kanatzidis, M. G. *Cryst. Growth Des.* **2012**, *12*, 3250. (e) Peters, J. A.; Cho, N. K.; Liu, Z.; Wessels, B. W.; Li, H.; Androulakis, J.; Kanatzidis, M. G. *J. Appl. Phys.* **2012**, *112*, 063702. (f) Cho, N. K.; Peters, J.A.; Liu, Z.; Wessels, B. W.; Johnsen, S.; Kanatzidis, M. G.; Song, J. H.; Jin, H.; Freeman, A. *Semicond. Sci. Tech.* **2012**, *27*, 015022. (g) Im, J.; Jin, H.; Li, H.; Peters, J. A.; Liu, Z. F.; Wessels, B. W.; Kanatzidis, M. G.; Freeman, A. J. *App. Phys. Lett.* **2012**, *101*, 202103. (h) Li, H.; Malliakas, C. D.; Liu, Z. F.; Peters, J. A.; Morris, C. D.; Zhao, L. D.; Wessels, B. W.; Freeman, A. J.; Kanatzidis, M. G. *Chem. Mater.* **2012**, *24*, 4434. (i) Liu, Z.; Peters, J. A.; Li, H.; Kanatzidis, M. G.; Wessels, B. W. *Semicond. Sci. Tech* **2013**, *28*, 015016. (j) Liu, Z. F.; Peters, J. A.; Wessels, B. W.; Johnsen, S.; Kanatzidis, M. G. *Nucl. Instrum. Meth. Phys. Sect. A* **2011**, *659*, 333.

(6) Malliakas, C. D.; Wibowo, A. C.; Liu, Z.; Peters, J. A.; Sebastian, M.; Jin, H.; Chung, D.-Y.; Freeman, A. J.; Wessels, B. W.; Kanatzidis, M. G. In *Proc. SPIE, Hard X-Ray, Gamma-Ray, and Neutron Detector Physics XIV*, San Diego, CA, Aug 12, 2012; SPIE: Bellingham, WA, 2012; p 85070F.

(7) Manfredotti, C.; Murri, R.; Quirini, A.; Vasanelli, L. *IEEE Trans. Nucl. Sci.* **1977**, *24*, 126.

(8) Matsumoto, M.; Hitomi, K.; Shoji, T.; Hiratate, Y. In *Nuclear Science Symposium Conference Record, 2001 IEEE* San Diego, CA, USA, 4−10 Nov 2001, IEEE: New Brunswick, NJ, **2001**; Vol. *4*, p 2344.

(9) Gits, S.; Authier, A. *J. Cryst. Growth* **1982**, *58*, 473.

(10) Berger, M. J. *XCOM Photon Cross Sections Database*; NIST Physics Laboratory: Gaithersburg, MA, 1998.

(11) Moller, C. K. *Nature* **1958**, *182*, 1436.

(12) (a) Hirotsu, S.; Harada, J.; Iizumi, M.; Gesi, K. *J. Phys. Soc. Jpn.* **1974**, *37*, 1393. (b) Sakata, M.; Nishiwaki, T.; Harada, J. *J. Phys. Soc. Jpn.* **1979**, *47*, 232. (c) Sakata, M.; Harada, J.; Cooper, M. J.; Rouse, K. D. *Acta Crystallogr., Sect. A* **1980**, *36*, 7. (d) Rodová, M.; Brožek, J.; Knížek, K.; Nitsch, K. *J. Therm. Anal. Calorim.* **2003**, *71*, 667.

(13) (a) Nitsch, K.; Hamplová, V.; Nikl, M.; Polák, K.; Rodová, M. *Chem. Phys. Lett.* **1996**, *258*, 518. (b) Babin, V.; Fabeni, P.; Nikl, M.; Pazzi, G. P.; Sildos, I.; Zazubovich, N.; Zazubovich, S. *Chem. Phys. Lett.* **1999**, *314*, 31. (c) Nikl, M.; Nitsch, K.; Mihóková, E.; Polák, K.; Fabeni, P.; Pazzi, G. P.; Gurioli, M.; Santucci, S.; Phani, R.; Scacco, A.; Somma, F. *Physica E* **1999**, *4*, 323. (d) Somma, F.; Nikl, M.; Nitsch, K.; Fabeni, P.; Pazzi, G. P. *J. Lumin.* **2001**, *94*−*95*, 169. (e) Sakuma, T.; Mutou, M.; Ohki, K.; Arai, M.; Takahashi, H.; Ishii, Y. *Solid State Ionics* **2002**, *154*−*155*, 237. (f) Kondo, S.-i.; Kakuchi, M.; Masaki, A.; Saito, T. *J. Phys. Soc. Jpn.* **2003**, *72*, 1789.

(14) (a) Chang, H., Y.; Park, H., C.; Matsuishi, K. *J. Korean Phys. Soc.* **2004**, *44*, 5. (b) Heidrich, K.; Künzel, H.; Treusch, J. *Solid State Commun.* **1978**, *25*, 887. (c) Kondo, S.; Suzuki, K.; Saito, T.; Asada, H.; Nakagawa, H. *Phys. Rev. B* **2004**, *70*, 205322.

(15) (a) Mizusaki, J.; Arai, K.; Fueki, K. *Solid State Ionics* **1983**, *11*, 203. (b) Narayan, R. L.; Sarma, M. V. S.; Suryanarayana, S. V. *J. Mater. Sci. Lett.* **1987**, *6*, 93. (c) Clark, S. J.; Donaldson, J. D.; Harvey, J. A. *J. Mater. Chem.* **1995**, *5*, 1813.

(16) $CsPbBr_3$:Cs1Pb1Br3, fw = 579.83 g/mol, orthorhombic, space group *Pnma* with a = 8.2440(6) Å, b = 11.7351(11) Å, c = 8.1982(8) Å, V = 793.13(12) Å^3, T = 293(2) K, Z = 4, R_1 [$I > 2\sigma(I)$] = 0.0376, *wR*2 (F^2, all data) = 0.0891.

(17) (a) Kroumova, E.; Aroyo, M. I.; Perez-Mato, J. M.; Kirov, A.; Capillas, C.; Ivantchev, S.; Wondratschek, H. *Phase Transitions* **2003**, *76*, 155. (b) Sheldrick, G. *Acta Crystallogr., Sect. A* **2008**, *64*, 112. (c) Spek, A. L. *Acta Crystallogr. Sect. D* **2009**, *65*, 148.

(18) Petricek, V.; Dusek, M.; Palatinus, L. *JANA2006*; Institute of Physics: Praha, Czech Republic, 2006.

(19) (a) Heidrich, K.; Schäfer, W.; Schreiber, M.; Söchtig, J.; Trendel, G.; Treusch, J.; Grandke, T.; Stolz, H. J. *Phys. Rev. B* **1981**, *24*, 5642. (b) Murtaza, G.; Ahmad, I. *Phys. B* **2011**, *406*, 3222.

(20) (a) Taguchi, T.; Shirafuji, J.; Inuishi, Y. *Phys. Status Solidi B* **1975**, *68*, 727. (b) Schmidt, T.; Lischka, K.; Zulehner, W. *Phys. Rev. B* **1992**, *45*, 8989.

(21) Many, A. *J. Phys. Chem. Solids* **1965**, *26*, 575.

(22) Luke, P. N. *Appl. Phys. Lett.* **1994**, *65*, 2884.

(23) Jacoboni, C.; Canali, C.; Ottaviani, G.; Quaranta, A. A. *Solid State Electron.* **1977**, *20*, 77.

(24) Cho, H. Y.; Lee, J. H.; Kwon, Y. K.; Moon, J. Y.; Lee, C. S. *J. Instrum.* **2011**, *6*, C01025.